Materials Performance and Characterization

doi:10.1520/MPC20170002 / Vol. 6 / No. 5 / 2017 / available online at www.astm.org

U. V. Nayak,[1] G. Ramesh,[1] and K. N. Prabhu[2]

Assessment of Spatiotemporal Heat Flux during Quenching in TiO_2 and AlN Nanofluids

Reference

Nayak, U. V., Ramesh, G., and Prabhu, K. N., "Assessment of Spatiotemporal Heat Flux during Quenching in TiO_2 and AlN Nanofluids," *Materials Performance and Characterization*, Vol. 6, No. 5, 2017, pp. 745–756, https://doi.org/10.1520/MPC20170002. ISSN 2379-1365

ABSTRACT

In the present work, spatiotemporal heat flux transients were estimated during quenching of an Inconel 600 alloy probe in water-based titanium dioxide (TiO_2) and aluminum nitride (AlN) nanofluids that have nanoparticle concentrations varying from 0.001 to 0.5 vol. %. The results showed reduced peak heat flux and a longer vapor phase stage during quenching with nanofluids compared to quenching with water. The peak heat flux for quenching in nanofluids was lowered with increase in the nanoparticle concentration. Quenching with TiO_2 nanofluids resulted in slower heat extraction compared to quenching in AlN nanofluids at higher concentrations. Quenching with nanofluids resulted in a more uniform quench compared to quenching with water because of the reduction in the rewetting period.

Keywords

quenching, nanofluids, spatiotemporal heat flux, rewetting

Manuscript received January 12, 2017; accepted for publication April 28, 2017; published online October 3, 2017.

[1] Department of Metallurgical and Materials Engineering, N.I.T.K., Surathkal, Mangalore-575025, India

[2] Department of Metallurgical and Materials Engineering, N.I.T.K., Surathkal, Mangalore-575025, India (Corresponding author), e-mail: prabhukn_2002@yahoo.co.in

Introduction

Quench hardening of steel, in general, involves heating it to an austenitizing temperature followed by cooling in a suitable quench medium. Water is the most commonly available, inexpensive, and eco-friendly quench medium. However, its application is restricted because quenching with water results in undesired distortions and crack formations that render the heat-treated metal useless. To counter these adverse effects,

researchers in the past had resorted to raising the temperature of the water. The result of increased water temperature led to minimizing the ill effects of quenchant. Nevertheless, the consequence of elevated water temperature caused the strength of the processed metal to be lower than expected and resulted in soft spots due to a non-uniform quench.

Nanofluids, obtained by combining nanometer-sized substances with a carrier liquid, were first conceived by Choi [1] and were first employed by Prabhu and Fernandes [2] as a quench medium for industrial heat treatment. Quenching Inconel in water-based nano-sized alumina particles of 20 wt. % concentration lowered the peak heat transfer coefficient by about 124 W/m^2K compared to water [2]. Zupan et al. [3] investigated the effect of the addition of titanium dioxide (TiO_2) in water and alumina nanoparticles in 30 % polyalkylene glycol (PAG) solution. Their study showed higher cooling rates with water-TiO_2 nanofluids and earlier disruption of full film boiling with PAG-water-alumina nanofluid. Kim et al. [4] showed that the quench characteristics of water-based alumina nanofluids were similar to that of deionized water. According to them, the only influence nanoparticles had during quenching was their deposition on the metal surface that caused destabilization of the vapor phase stage and consequently resulted in the early occurrence of the nucleate boiling stage. Babu and Kumar [5] used water-based chemically treated carbon nanotube (TCNT) nanofluids to study quench characteristics relative to deionized water. Their findings showed peak flux obtained was the highest with 0.5 wt. % CNT nanofluids and was about 1 MW higher than that obtained with water. Their study also showed deteriorated heat transfer behavior for nanofluids. The peak heat flux was lowered by about 42 % when the 0.5 wt. % nanofluids quench medium was agitated compared to quenching under still conditions. Ciloglu et al. [6] showed that quenching with copper (II) oxide (CuO), aluminum oxide (Al_2O_3), titania (TiO_2) and silicon dioxide (SiO_2)-water nanofluids was similar to quenching with water. Repeat quench experiments using unclean (nanoparticles deposited from presiding experiments) quench probes immersed in nanofluids showed enhanced cooling performance because of improved wettability that resulted from the modified surface morphology of the probe due to deposition. The cooling performance of water-clay nanofluids of concentrations 0.001, 0.01, and 0.1 vol. % was assessed by Ramesh and Prabhu [7]. The results of their experiments showed decreased peak cooling rates during quenching with nanofluids compared to water. They reported the formation of a porous layer at the metal/quenchant interface during quenching that would extend the vapor phase stage duration, which subsequently manifested in lower peak heat flux and increased quench time during quenching with nanofluids. Quenching with alumina nanoparticles at a concentration of 0.05 vol. % had shown a 16 % increase in the peak cooling rate compared to water [8]. They observed that a shorter vapor phase stage duration was realized during quenching with 0.05 vol. % alumina nanofluid. The above outcomes clearly suggest that it is possible to alter the cooling performance of water with the addition of nanoparticles.

In the present investigation, titania and aluminum nitride (AlN) nanoparticles dispersed in distilled water in concentrations varying from 0.001 to 0.5 vol. % were used as quench media. The cooling performance of nanofluids was assessed with the aid of an Inconel 600 alloy quench probe conforming to ISO 9950, *Industrial quenching oils – Determination of cooling characteristics – Nickel-alloy probe test method* [9]. Heat flux transients were estimated along the probe surface by using inverse heat transfer software package. Their rewetting characteristics were assessed by utilizing the calculated cooling curve obtained at the surface of the probe.

Experimental Work

NANOFLUID PREPARATION

AlN and titania (20 nm) nanopowders were purchased from Reinste Nano Ventures Pvt. Ltd., Noida, India and Sigma-Aldrich Co., India respectively. A two-step method of preparation consisting of the addition of nanoparticles to distilled water was followed to obtain 0.01, 0.05, 0.1, and 0.5 vol. % concentrated water-nanofluids. The nanofluids thus obtained were homogenized by stirring. A magnetic stirrer operating at a speed of 500 r/min for about 10 h was used for this purpose.

A Brookfield viscometer (DV-III Ultra) was used to measure the viscosity of the quench media. The viscosity measurements were carried out at 30 ± 2°C in an ultralow adapter with an accompanying spindle that utilizes 16 mL of the test fluid.

EXPERIMENTAL SETUP

The quenching experiment was carried out with a ø 12.5 mm by 60 mm quench probe machined from Inconel 600 alloy. To accommodate thermocouples, 1-mm-diameter holes were drilled in the probe at locations shown in Fig. 1 using electrical discharge machining (EDM). The hole depths were 7.5, 22.5, 30, 37.5, 45, 52.5, and 40 mm near the surface, and the geometric center of the probe was at 30 mm. The holes near the surface were spaced 45° apart and were drilled at a distance of 2 mm from the surface of the probe. Temperature measurements were obtained using calibrated K-type thermocouples that were press-fitted into each of these holes. The probe instrumented with thermocouples was then placed in a vertical tubular furnace as shown in Fig. 2. This furnace, with its top end covered with insulating material and the bottom end left open, was heated to 850°C. On attaining this temperature, the hot probe was immersed in 2 L of quench medium that had been placed in a glass container, positioned below the bottom end of the furnace. All the thermocouples were connected to a data logger (NI 9213) via K-type compensating cables. The data logger was interfaced to a personal computer for recording and storing temperature data. The data were recorded at an interval of 0.1 s. At the start of each experiment, the temperature of the liquid quench medium

FIG. 1

Computer-aided drawing of the Inconel probe showing thermocouple locations.

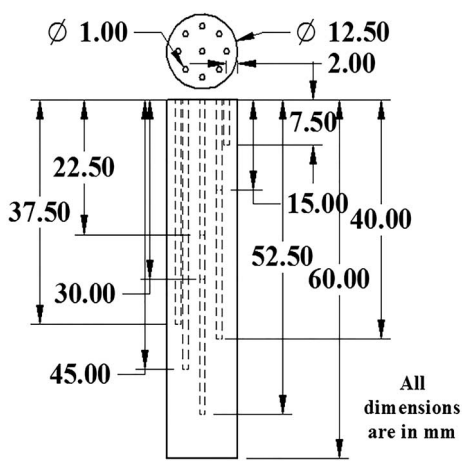

FIG. 2

Schematic of the quench setup.

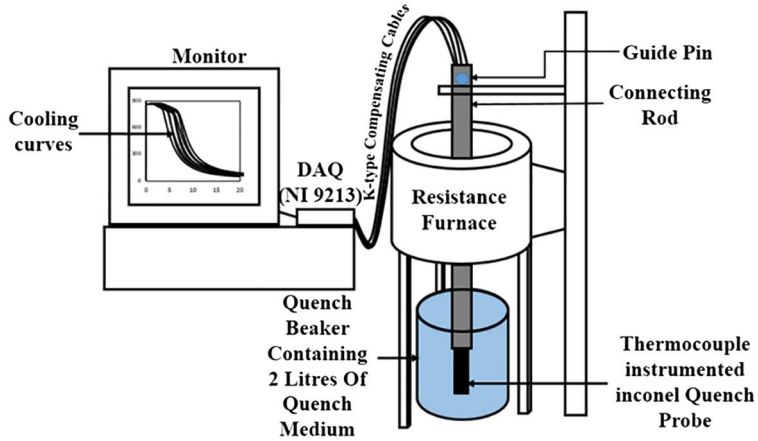

was about 28 ± 2°C. Quench experiments were performed under still conditions. The probe was thoroughly cleaned with acetone and rinsed with water after each experiment.

HEAT FLUX ESTIMATION

The spatially dependent surface heat flux transients were estimated by inverse heat conduction technique using thermo-mechanical-metallurgical finite elements (TmmFe) software (Thermet Solutions, Pvt. Ltd., Bangalore). This technique uses the two-dimensional transient heat conduction given below:

$$\frac{\partial}{\partial r}\left(\lambda r\frac{\partial T}{\partial r}\right)+\frac{\partial}{\partial z}\left(\lambda\frac{\partial T}{\partial z}\right)=\rho C_p\frac{\partial T}{\partial t} \tag{1}$$

where λ represents the thermal conductivity of Inconel alloy, r the radius of the probe, T the temperature, z the height, ρ the density, and C_p the specific heat. This two-dimensional governing equation was solved inversely by using the following initial and boundary conditions according to the procedure detailed in Ref. [10] to obtain the metal/quenchant interfacial heat flux transient:

Initial condition:

$$T(r,z)=T_i \quad \text{at} \quad t=0 \tag{2}$$

and boundary conditions:

$$-\lambda\frac{\partial T}{\partial r}n_r-\lambda\frac{\partial T}{\partial z}n_z=q_k(r,z,t) \quad \text{on} \quad \Gamma_k; k=1,2,\ldots,\text{p}\ldots,1 \tag{3}$$

$$-\lambda\frac{\partial T}{\partial r}n_r-\lambda\frac{\partial T}{\partial z}n_z=0 \quad \text{on} \quad \Gamma' \tag{4}$$

The solution domain used for solving the unknown q heat fluxes inversely is shown in Fig. 3. The half symmetrical shape of quench probe A was discretized uniformly using four node quadrilateral elements. The total number of elements used was 3,575. The thermal

FIG. 3

Axisymmetric solution domain used in inverse heat conduction software.

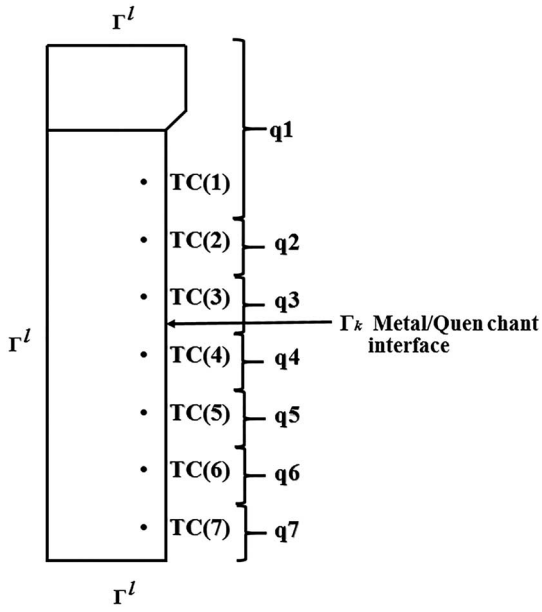

properties (Table 1) and the measured thermal history data (except H40) were provided as input to the software. The surface of the probe in contact with the liquid was divided into seven segments where q heat fluxes were estimated. The convergence limit for Gauss-Siedel iterations was set at 10^{-6}.

TABLE 1

Thermophysical properties of the Inconel 600 alloy quench probe [11].

Temperature (°C)	Thermal Conductivity k (Wm/K)	Specific Heat C_p (J/kgK)	Density ρ (kg/m^3)
50	13.4	451	-
100	14.2	467	-
150	15.1	-	-
200	16	491	-
250	16.9	-	-
300	17.8	509	-
350	18.7	-	-
323	-	-	8,400
373	-	-	8,370
400	19.7	522	-
450	20.7	-	-
473	-	-	8,340
500	21.7	591	-
573	-	-	8,300
673	-	-	8,270
700	25.9	597	-
773	-	-	8,230
800	-	602	-
873	-	-	8,190
900	30.1	611	-
973	-	-	8,150

Results and Discussion

Cooling curves obtained at the geometric center of the quench probe are shown in Fig. 4. The cooling rate curves as a function of temperature are also superimposed in this figure. The cooling curves exhibit the three characteristic modes of heat transfer: full film boiling, nucleate boiling, and convective cooling. These curves show that the duration of the vapor phase stage observed during quenching with water becomes longer with the addition of nanoparticles. Table 2 shows the critical cooling parameters obtained by analyzing the cooling curves. The vapor phase stage duration was increased about eight times during quenching with 0.01 vol. % AlN-water nanofluid compared with water. However, no relation was obtained between the amount of nanoparticle added to water and the duration of vapor phase stage because of the complex nature of Brownian motion that is associated with the dispersed nanoparticles. The peak cooling rate was highest during quenching with water followed by 0.01 vol. % TiO_2, with 0.05 and 0.1 vol. % AlN showing similar cooling rates of about 155°C/s. The lowest cooling rate was obtained with 0.5 vol. % TiO_2 nanofluid (reduced by 38 % compared to water) and at the same concentration the peak rate during quenching with AlN was found to be 148°C/s. However, the temperature at which

FIG. 4

Cooling curves and their rates obtained at the geometric center of the quench probe during quenching with (a) AlN and (b) titania nanofluids of various concentrations.

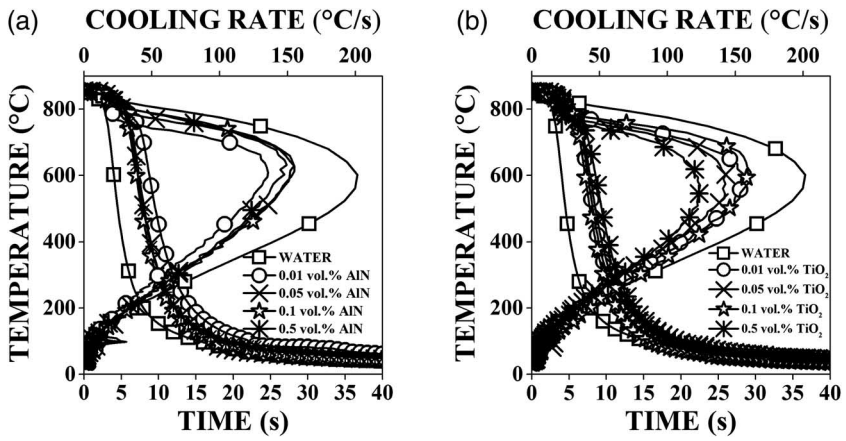

TABLE 2

Critical cooling parameters.

Quench media	$t_{A\text{-}B}$ (s)	CR_{max} (°C/s)	CR_{705} (°C/s)	CR_{550} (°C/s)	CR_{300} (°C/s)	CR_{200} (°C/s)	T_{maxcr} (°C)	$t_{705\text{-}260}$ (s)	$CR_{500\text{-}600}$ (°C/s)
Water	0.6	200.7	174.6	192.9	81.7	34.1	601.8	3.2	191.9
0.01 vol. % AlN	4.8	135.5	105.8	125.7	55.7	26.6	609.3	4.8	125.3
0.05 vol. % AlN	3.5	155.1	135.9	142.5	65.8	35.1	628.4	4.2	141.7
0.1 vol. % AlN	2.8	153.4	134.8	143.2	68.6	34.4	629.4	4.1	142.7
0.5 vol. % AlN	N/A	148.5	131.0	135.8	65.9	32.9	647.1	4.3	134.6
0.01 vol. % TiO_2	3.3	156.1	120.0	151.1	70.6	36.3	603.8	3.9	150.7
0.05 vol. % TiO_2	3.7	143	110.7	142.1	64.4	30.2	546.1	4.3	139.8
0.1 vol. % TiO_2	2.9	161	138.2	153.7	77.1	41.2	625.4	3.7	153.2
0.5 vol. % TiO_2	4.1	124	91.5	123.2	64.8	32.9	570.1	4.6	122.5

TABLE 3
Viscosity of quenchants.

Quench media	Viscosity (cPs)
Water	0.97
0.01 vol. % AlN	1.44
0.05 vol. % AlN	1.03
0.1 vol. % AlN	1.01
0.5 vol. % AlN	0.99
0.01 vol. % TiO_2	1.03
0.05 vol. % TiO_2	0.96
0.1 vol. % TiO_2	1.04
0.5 vol. % TiO_2	1.09

the peak cooling rate occurs is higher with nanofluids compared to water and is beneficial because it would aid in a lower propensity towards pearlitic transformation. Cooling rates at 705°C, 550°C, 300°C, and 200°C represent the cooling rates obtained in the pearlite transformation region (705°C), the nose of the continuous cooling transformation diagram (550°C), martensite start (300°C), and martensite finish (200°C) temperatures, respectively, for most steel. The cooling rates at these temperatures were observed to be lower for nanofluids compared to water. The reduction in cooling rates for nanofluids compared to water is due to their increased viscosities. Table 3 shows the measured viscosity of nanofluids and water.

Fig. 5 shows the cooling curves measured using the near-surface thermocouples at various locations in the probe during quenching with water and nanofluids. The cooling curves obtained are similar in nature to the curves observed at the geometric center of the probe. From these curves, it is clearly seen that the vapor phase stage that initially encapsulates the probe surface is the least at the T7 location in all the experiments. Also, the duration of the vapor phase stage increases progressively from T7 to T1. This implies that in each of the experiments, the vapor phase breaks at the bottom location of the quench probe and ascends along the probe surface. It also implies the presence of a rewetting front that forms a boundary between the vapor phase and the nucleate boiling phase during quenching. The heat flux estimated at the metal/quenchant interface utilizing these near-surface temperature data is shown in Fig. 6. The nature of the flux curve is the same for both water and nanofluids. Each of the flux curves has an initial plateau region because of the vapor phase stage. The flux during this stage is nearly constant following the first critical heat flux, as shown by a local maximum. At the instant the vapor phase stage breaks, the flux begins to increase with the quench medium experiencing nucleate boiling. During the nucleate boiling stage, the flux attains its maximum value. An order of difference exists between the heat flux obtained during the nucleate boiling stage and other stages as seen from the figures. With continued heat transfer, the flux begins to drop from its global maximum and finally enters the convective cooling stage. The heat flux during the beginning of the final convective stage has values higher than those obtained during the vapor phase stage. With further cooling, the heat flux drops and finally attains a constant value. It is clear from the spatiotemporal heat flux plots that the peak flux would be reduced with an increase in the concentration of nanomaterial in water. The peak heat flux obtained at various heat flux boundaries segments are shown in Table 4. Also, the time required for the completion of the quench operation would be longer during quenching

FIG. 5

Measured temperature in the Inconel probe at various locations TC (1), TC (2), TC (3), TC (4), TC (5), TC (6), and TC (7) during quenching in water and AlN and TiO_2 nanofluids of various concentrations.

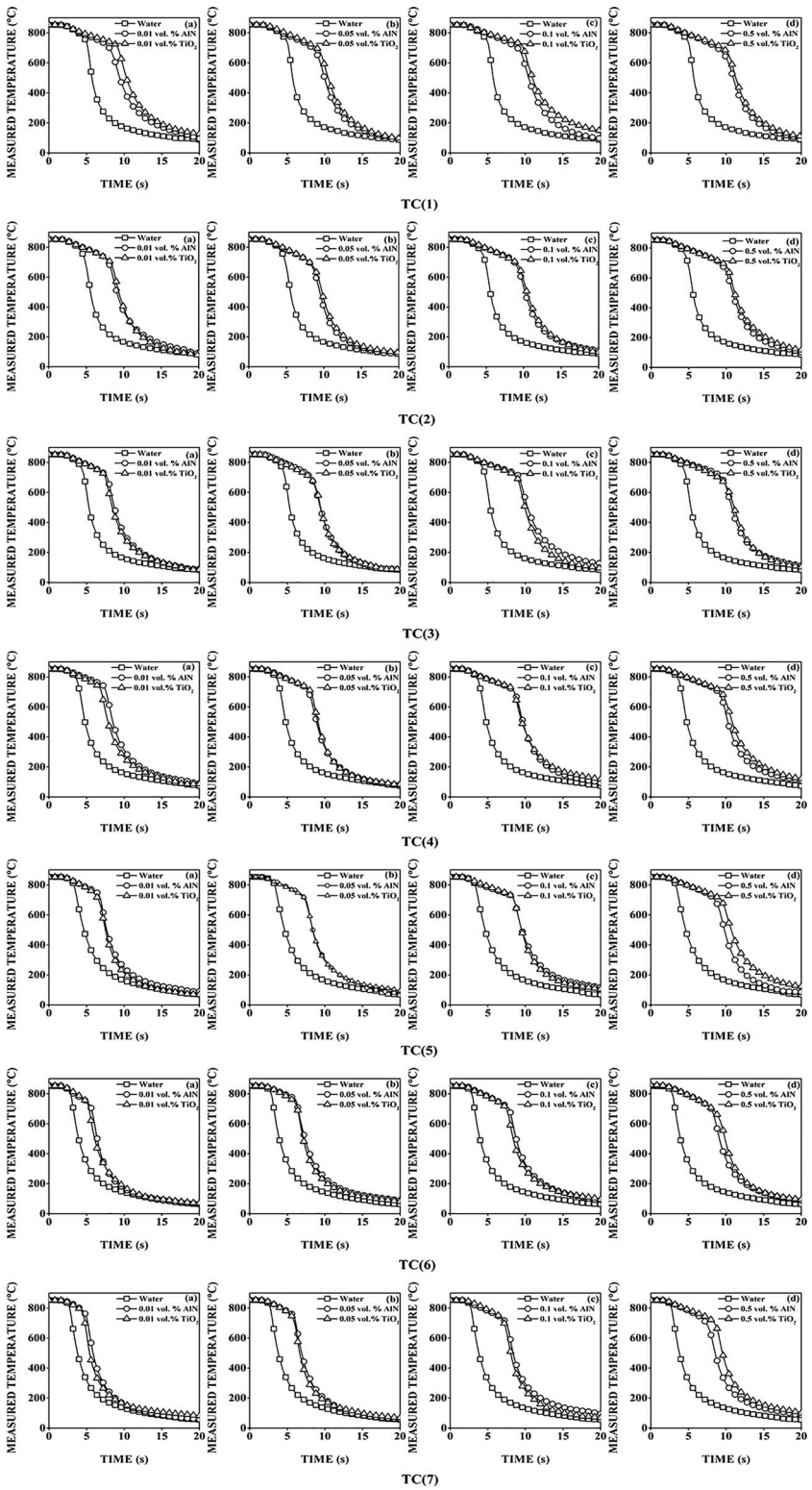

FIG. 6

Estimated heat flux transients at the interfacial boundary segments q1, q2, q3, q4, q5, q6, and q7 of the Inconel probe during quenching with water and nanofluids.

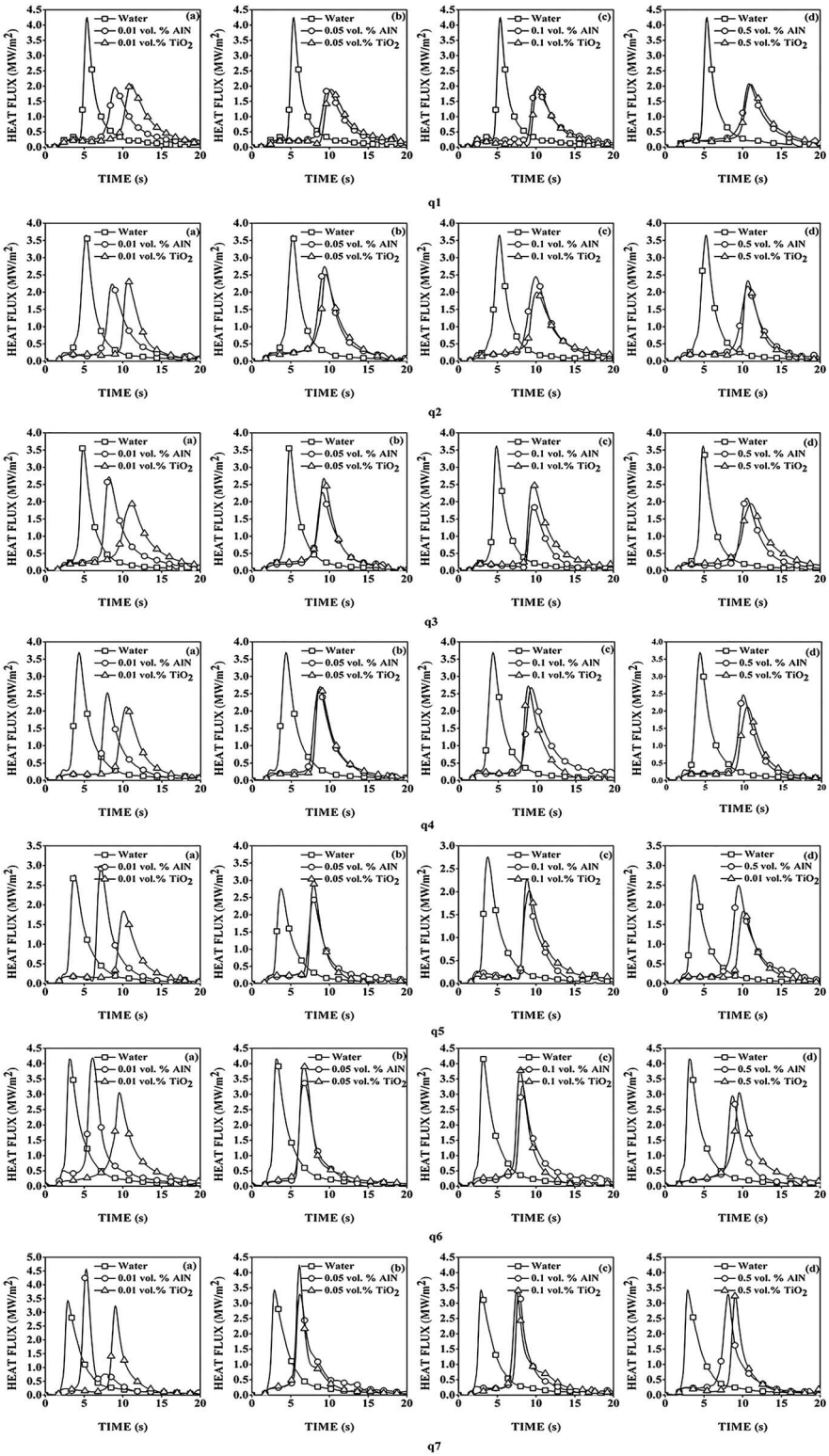

TABLE 4
Peak heat flux obtained at various interfacial boundary segments.

	Peak Heat Flux (MW/m^2) at Various Boundary Segments						
Quench media	q1	q2	q3	q4	q5	q6	q7
Water	4.25	3.65	3.62	3.69	2.76	4.15	3.44
0.01 vol. % AlN	1.96	2.23	2.72	2.53	2.93	4.18	4.57
0.05 vol. % AlN	1.91	2.74	2.27	2.65	2.44	3.36	3.29
0.1 vol. % AlN	1.92	2.45	1.86	2.67	2.29	3.28	3.45
0.5 vol. % AlN	2.08	2.17	2.10	2.47	2.49	2.95	3.30
0.01 vol. % TiO_2	2.05	2.33	1.94	2.12	1.84	3.05	3.23
0.05 vol. % TiO_2	1.89	2.52	2.68	2.70	2.90	3.94	4.24
0.1 vol. % TiO_2	1.99	2.00	2.51	2.72	2.02	3.78	3.36
0.5 vol. % TiO_2	2.05	2.33	1.94	2.12	1.84	3.05	3.23

with nanofluids compared to water. Fig. 7 shows the fraction of heat removed by the quench medium as a function of time during quenching in various nanofluids. The following methodology was used to obtain fraction heat removed:

- The time required for the TC(1) thermocouple to reach 60°C during quenching was noted and was taken as the base value.
- The area under each heat flux curve up to the base value was obtained.
- The average area was computed and each value was normalized with the base value to obtain the fraction of heat removed.

The heat was removed at the slowest rate during quenching with 0.5 % volume fraction nanofluid. In Fig. 7, it is observed that 0.05 and 0.1 vol. % AlN took nearly the same time to extract a given amount of heat. The time taken to extract about 60 % heat increases by two-fold in the case of 0.01 vol. % nanofluid relative to water. Beyond this concentration, the time required to remove a given amount of heat by nanofluids was found to be linearly related to the time taken by 0.01 vol. % nanofluid for removal of that given amount of heat. AlN and TiO_2 nanofluids take nearly the same time to remove a given fraction of

FIG. 7 Time for specified heat removed from the quench probe for (a) AlN and (b) TiO_2 nanofluids of various concentrations.

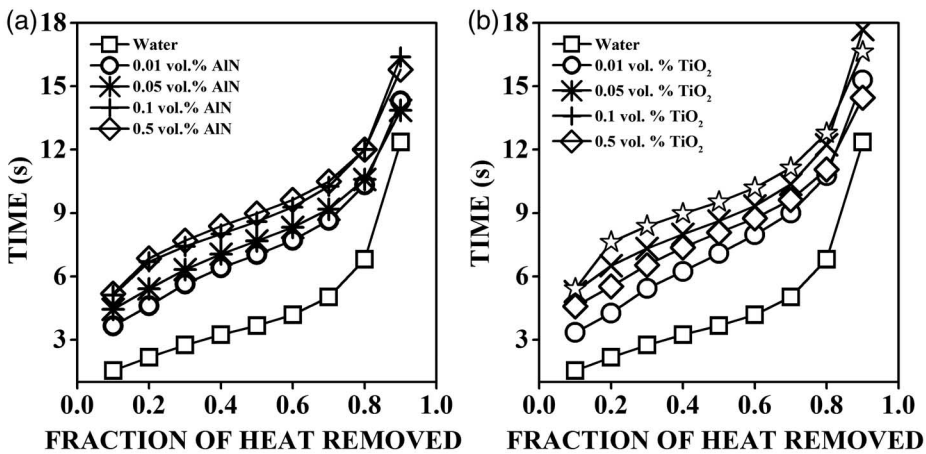

heat at concentrations of 0.01, 0.05, and 0.1 vol. %, whereas it takes longer for titania nanofluid at a concentration of 0.5 vol. % to remove heat compared to AlN.

Average rewetting time was obtained on the surface of the probe using temperature data extracted at locations corresponding to the near surface thermocouples. It was observed that quenching with water required 2.85 s for the rewetting front to reach a height of 7.5 mm from the top end of the probe. The same time was found to be 2.57, 4.1, 5.07, and 5.01 s for AlN nanofluids with concentrations varying from 0.01 to 0.5 vol. % and 3.9, 4.34, 5.4, and 4.78 s for 0.01, 0.05, 0.1, and 0.5 vol. % TiO_2 nanofluids, respectively. These times suggest that the time taken by nanofluids to rewet the probe increased with concentration. The deviation in the rewetting time obtained at the seven locations at the surface showed the value of 1.4 s for water. The corresponding values were 1.1, 1.4, 1.9, and 1.3 s for 0.01 to 0.5 vol. % AlN nanofluids. For TiO_2 nanofluids of concentrations ranging from 0.01 to 0.5 vol. %, the deviation in rewetting times were found to be 2.1, 1.9, 1.8, and 1.0 s respectively. These results show that 0.01 vol. % AlN nanofluid and 0.5 vol. % TiO_2 nanofluid extracted heat more uniformly compared to water. Moreover, it also implies that once rewetting begins, it proceeds faster during quenching with nanofluids, especially at higher concentrations.

Conclusions

The following are the conclusions drawn from this study:

- Quenching with nanofluids resulted in extended vapor phase stage duration.
- The addition of nanoparticles increased the viscosity of water, leading to lower peak cooling rate compared to water.
- Heat extraction was slowest with 0.5 vol. % TiO_2 nanofluid.
- Nanoparticle additions affected the rewetting behavior of water and caused faster rewetting front movement.

ACKNOWLEDGMENTS

One of the authors (KNP) thanks the Science and Engineering Research Board (SERB), Department of Science and Technology (DST), New Delhi, India for the research grant.

References

[1] Choi, S. U. S. and Eastman, J. A., "Enhancing Thermal Conductivity of Fluids with Nanoparticles," presented at the *International Mechanical Engineering Congress and Exhibition*, San Francisco, CA, November 12–17, 1995, USDOE, Washington, D.C., pp. 1–8, https://web.archive.org/save/_embed/https://www.osti.gov/scitech/biblio/196525 (accessed 2 Sept. 2017).

[2] Prabhu, K. N. and Fernandes, P., "Nanoquenchants for Industrial Heat Treatment," *J. Mater. Eng. Perform.*, Vol. 17, No. 1, 2008, pp. 101–103, https://doi.org/10.1007/s11665-007-9124-1

[3] Zupan, J., Filetin, T., and Landek, D., "Cooling Characteristics of the Water Based Nanofluids in Quenching," presented at the *International Conference MATRIB: Materials, Tribology, Recycling*, Vela Luka, Croatia, June 29–July 01, 2011, Croatian Society for Materials and Tribology, Zagreb, Croatia, pp. 575–584, https://web.archive.org/web/20170902033026/http://titan.fsb.hr/~tfiletin/en/data/_uploaded/clanci/65_Zupan_Filetin_Landek.pdf (accessed 26 April 2017).

[4] Kim, H., Buongiorno, J., Hu, L. W., McKrell, T., and DeWit, G., "Experimental Study on Quenching of a Small Metal Sphere in Nanofluids," presented at the *International*

Mechanical Engineering Congress and Exposition, Boston, MA, October 31–November 6, 2008, ASME International, New York, pp. 1839–1844, https://doi.org/10.1115/IMECE2008-67788

[5] Babu, K. and Kumar, T. S. P., "Optimum CNT Concentration and Bath Temperature for Maximum Heat Transfer Rate During Quenching in CNT Nanofluids," *J. ASTM Int.*, Vol. 9, No. 5, 2012, pp. 1–12, https://doi.org/10.1520/JAI104442

[6] Ciloglu, D., Bolukbasi, A., and Comakli, K., "Effect of Nanofluids on the Saturated Pool Film Boiling," *Int. J. Chem. Mole. Nuc. Mater. Metall. Eng.*, Vol. 6, No. 7, 2012, pp. 1122–1124, https://web.archive.org/web/20170902032759/https://www.waset.org/Publications?q=effect+of+nanofluids+on+the+saturated+pool+film+boiling&search=Search (accessed 26 April 2017).

[7] Ramesh, G. and Prabhu, K. N., "Development of Clay Based Nanofluids for Quenching," presented at the *Sixth International Conference on Quenching and Control of Distortion Conference Including the fourth International Distortion Engineering Conference*, Chicago, IL, September 9–13, 2012, ASM International, Materials Park, OH, pp. 308–318.

[8] Ramesh, G. and Prabhu, K. N., "Effect of Addition of Aluminum Nanoparticles on Cooling Performance and Quench Severity of Water during Immersion Quenching," *J. ASTM Int.*, Vol. 9, No. 5, 2012, pp. 1–9, https://doi.org/10.1520/JAI104404

[9] ISO 9950, *Industrial Quenching Oils – Determination of Cooling Characteristics – Nickel-Alloy Probe Test Method*, ISO, Geneva, Switzerland, iso.org

[10] Kumar, T. S. P., "A Serial Solution for the 2-D Inverse Heat Conduction Problem for Estimating Multiple Heat Flux Components," *Num. Heat Trans. B.*, Vol. 45, No. 6, 2004, pp. 541–563, https://doi.org/10.1080/10407790490277940

[11] Penha, R. N., Canale, L. C. F., Totten, G. E., Sarmiento, G. S., and Ventura, J. M., "Simulation of Heat Transfer and Residual Stresses from Cooling Curves Obtained in Quenching Studies," *J. ASTM Int.*, Vol. 3, No. 5, 2006, pp. 1–14, https://doi.org/10.1520/JAI13614